

## Role of $\text{Ca}^{2+}$ for Inactivation of N-type Calcium Current in Rat Sympathetic Neurons

Yong Sook Goo\* and Keith S. Elmslie†

\*Department of Physiology, Chungbuk National University Medical School, Cheongju, Korea 361-763

†Department of Physiology, Tulane University Medical School, New Orleans, LA 70112

The voltage-dependence of N-type calcium current inactivation is U-shaped with the degree of inactivation roughly mirroring inward current. This voltage-dependence has been reported to result from a purely voltage-dependent mechanism. However,  $\text{Ca}^{2+}$ -dependent inactivation of N-channels has also been reported. We have investigated the role of  $\text{Ca}^{2+}$  in N-channel inactivation by comparing the effects of  $\text{Ba}^{2+}$  and  $\text{Ca}^{2+}$  on whole-cell N-current in rat superior cervical ganglion neurons. For individual cells inactivation was always larger in  $\text{Ca}^{2+}$  than in  $\text{Ba}^{2+}$  even when internal EGTA (11 mM) was replaced with BAPTA (20 mM). The inactivation vs. voltage relationship was U-shaped in both divalent cations. The enhancement of inactivation by  $\text{Ca}^{2+}$  was inversely related with the magnitude of inactivation in  $\text{Ba}^{2+}$  as if the mechanisms of inactivation were the same in both  $\text{Ba}^{2+}$  and  $\text{Ca}^{2+}$ . In support of this idea we could separate fast ( $\tau \sim 150$  ms) and slow ( $\tau \sim 2500$  ms) components of inactivation in both  $\text{Ba}^{2+}$  and  $\text{Ca}^{2+}$  using 5 sec voltage steps. Differential effects were observed on each component with  $\text{Ca}^{2+}$  enhancing the magnitude of the fast component and the speed of the slow component. The larger amplitude of fast component indicates that the more channels inactivate via this pathway with  $\text{Ca}^{2+}$  than with  $\text{Ba}^{2+}$ , but the stable time constants support the idea the fast inactivation mechanism is identical in  $\text{Ba}^{2+}$  and  $\text{Ca}^{2+}$ . The results do not support a  $\text{Ca}^{2+}$ -dependent mechanism for fast inactivation. However, the  $\text{Ca}^{2+}$ -induced acceleration of the slowly inactivating component could result from a  $\text{Ca}^{2+}$ -dependent process.

**Key Words :** N-current, Whole-cell patch-clamp, Voltage-clamp, Voltage-dependent inactivation

### INTRODUCTION

Influx of  $\text{Ca}^{2+}$  through N-type calcium channels triggers neurotransmitter release at a variety of central and peripheral synapses.<sup>1)</sup> Neurotransmitter-induced inhibition of N-current has been shown to reduce neurotransmitter release.<sup>2-7)</sup> Inactivation provides another mechanism by which N-channel activity can be reduced. Indeed, it was recently been concluded that accumulated calcium chan-

nel inactivation during a train of action potentials contributes to posttetanic depression.<sup>8)</sup>

Early studies on inactivation focused on invertebrate calcium channels and vertebrate L-type calcium channels. These studies described two mechanisms of inactivation: voltage-dependent<sup>9-11)</sup> and  $\text{Ca}^{2+}$ -dependent.<sup>10-15)</sup> The voltage-dependent mechanism induces a monotonic decrease in current with increasing voltage, similar to the classic type of voltage-dependent inactivation first described by Hodgkin and Huxley.<sup>16)</sup> In  $\text{Ca}^{2+}$ -dependent inactivation, the rate and magnitude of inactivation depends on the internal  $\text{Ca}^{2+}$  concentration (near the channel). Thus, inactivation is correlated with current amplitude. This results in a U-shaped inactivation vs. voltage relation where inactivation is maximal at the voltage generating peak current and decreases as current becomes smaller at more depolarized and hyperpolarized voltages. Eckert and Chad<sup>17)</sup> showed that  $\text{Ca}^{2+}$ -dependent inactivation was attenuated when  $\text{Ca}^{2+}$  is re-

Submitted February 10, 2003, accepted March 7, 2003

This work was supported by grant No. R05-2001-000-00620-0 from the Basic Research Program of the Korea Science & Engineering Foundation to Y.S. Goo and with grants from LEQSF and NIH NINDS to K.S. Elmslie.

Corresponding autor: Yong Sook Goo, Department of Physiology, Chungbuk National University Medical School, Cheongju, Korea 361-763

Tel: 82-43-261-2870, Fax: 82-43-272-1603

Email: ysgoo@med.chungbuk.ac.kr

placed by  $\text{Ba}^{2+}$  or by monovalent cations, and can be prevented by buffering intracellular  $\text{Ca}^{2+}$ . However, the effect of buffering can be small in some preparations.<sup>10</sup> Voltage and  $\text{Ca}^{2+}$ -dependent mechanisms of inactivation have been shown to coexist in some calcium channels.<sup>10, 11</sup>

In N-type  $\text{Ca}^{2+}$  channels, the mechanisms of inactivation are more controversial. One reason for the controversy is that the inactivation vs. voltage relationship is U-shaped. Superficially this appears to argue for a  $\text{Ca}^{2+}$ -dependent mechanism. However, several properties of this inactivation deviate from predictions based on a  $\text{Ca}^{2+}$ -dependent mechanism. For example, the magnitude of inactivation is not strongly correlated with current amplitude, since substantial inactivation can be observed at voltages that generate little or no current.<sup>18-20</sup> In addition, the U-shaped inactivation vs. voltage relationship is observed when  $\text{Ca}^{2+}$  is replaced by  $\text{Ba}^{2+}$ .<sup>18, 20</sup> These differences from the  $\text{Ca}^{2+}$ -dependent hypothesis lead several investigators to propose unique voltage-dependent mechanisms for N-channel inactivation.<sup>18, 20</sup> Patil et al.<sup>20</sup> recently showed that a model where channels inactivated preferentially from intermediate closed states on the pathway to channel opening could explain the properties of N-channels inactivation. An analysis of gating currents supported predictions of the preferential closed state inactivation model.<sup>21</sup> A similar model has been proposed to explain the U-shaped inactivation vs. voltage relation for several potassium channels.<sup>22, 23</sup> Klemic et al.<sup>23</sup> termed this type of inactivation U-type to distinguish it from N-type and P/C-type inactivation. The existence of U-type inactivation in both calcium and potassium channels supports the idea that  $\text{Ca}^{2+}$  influx is not a requirement.

However,  $\text{Ca}^{2+}$  does have effects on N-channel inactivation. Increasing the external  $\text{Ca}^{2+}$  concentration can increase inactivation particularly when the concentration of intracellular  $\text{Ca}^{2+}$  buffering (EGTA or BAPTA) is low.<sup>19</sup> In addition, experiments using long depolarizations (3 sec) showed that more inactivation was observed during increased  $[\text{Ca}^{2+}]$  even with 10 mM EGTA.<sup>24</sup> These results were used to argue in favor of a  $\text{Ca}^{2+}$ -dependent mechanism for inactivation. Perhaps

the most compelling observation in support of a  $\text{Ca}^{2+}$ -dependent mechanism was that fast inactivation was absent when N-channels passed monovalent cations instead of divalent cations.<sup>19</sup> Recently further supporting evidence has been obtained from measurements of gating current. Shirokov<sup>25</sup> demonstrated U-shaped inactivation vs. voltage relation in N-channel gating current only when  $\text{Ca}^{2+}$  was allowed to permeate the channel. Inactivation increased monotonically with voltage when calcium currents were blocked by a combination of  $\text{Co}^{2+}$  and  $\text{Gd}^{2+}$ .

We have examined N-channel inactivation in rat superior cervical ganglion neurons to determine the effect of  $\text{Ca}^{2+}$ . To ensure in this paper that gross changes in internal  $\text{Ca}^{2+}$  concentration would not interfere with our measurement of inactivation, we have recorded currents using high internal concentrations of  $\text{Ca}^{2+}$  chelators (11 mM EGTA or 20 mM BAPTA). We show that  $\text{Ca}^{2+}$  can enhance calcium current inactivation and that the major calcium channel type affected is the N-type channel. This  $\text{Ca}^{2+}$ -induced enhancement resulted from an increase in the amplitude of the fast component and an increase in the speed of the slow component of inactivation. In the next paper, we examine the effect of changes in  $\text{Ca}^{2+}$  and  $\text{Ba}^{2+}$  concentration on inactivation. We believe that our data as well as those of other investigators can be explained if divalent cations are required for fast inactivation of N-channels. Our hypothesis differs from "classic"  $\text{Ca}^{2+}$ -dependent inactivation in two ways. First, both  $\text{Ca}^{2+}$  and  $\text{Ba}^{2+}$  are effective at triggering fast U-type inactivation. Second, divalent cation permeation is not required for fast U-type inactivation.

A preliminary report of some of these results has appeared in abstract form.<sup>26</sup>

## METHODS

### 1. Cell isolation procedure

Superior cervical ganglion (SCG) neurons were acutely isolated from adult Sprague Dawley rats (150-350 g) as described previously.<sup>27</sup> Briefly, rats were anes-

thetized with ether, decapitated and the heads placed in iced Hank's balanced salt solution. Neurons were dissociated from the isolated ganglia by enzymatic digestion followed by vigorous shaking. The enzymatic digestion was stopped by the addition of 10% fetal calf serum to the media. The dissociated cells were plated in 35 mm culture dishes and stored in a humidified atmosphere at 4°C (for up to 30 hrs) until use.

## 2. Electrophysiological recording

The neurons were voltage-clamped using the whole-cell configuration of the patch-clamp technique. Electrodes were fabricated from Corning 7740 glass (I.D. 0.90 mm, O.D. 1.5 mm, Garner Glass Co. Claremont, CA) using a Flaming/Brown P-87 pipette puller (Sutter Instrument Co., San Rafael, CA) and had resistances of 1-2 M $\Omega$  producing series resistance ( $R_s$ ) of  $3.52 \pm 1.13$  (mean  $\pm$  S.D.,  $n=70$ ). Series resistance was compensated by at least 80%. Membrane currents were recorded using an Axopatch 200A amplifier (Axon Instruments, Foster City, CA.) and digitized with a 12-bit A/D converter (GW Instruments Inc., Cambridge, MA) following analog filtering with the amplifier's 4 pole low pass Bessel filter. The digitization rate was at least 5 times the filter frequency. All experiments were conducted at room temperature.

## 3. Solutions

The high  $Cl^-$  internal solution contained in mM: 120 N-methyl-D-glucamine (NMG)-Cl, 10 tetraethylammonium (TEA)-Cl, 11 NMG2-EGTA, 10 NMG-HEPES, 1  $CaCl_2$ , 6  $MgCl_2$ , 2  $Li_3GDP-\beta-S$ , 14 creatine phosphate and 5  $Tris_2ATP$ . The high  $Cl^-$  external solution contained (mM) 140 TEA-Cl, 10 NMG-HEPES, 5  $BaCl_2$  or 5  $CaCl_2$ , 1  $MgCl_2$  and 15 glucose. The pH of both solutions was adjusted to 7.4 using NMG base. 2 mM  $Li_3GDP-\beta-S$  was used to block endogenous G-protein activation.

In low  $Cl^-$  internal solution, 120 NMG-Cl and 10 TEA-Cl were substituted to 125 NMG-OH, 20 TEA-OH, respectively and titrated with methanesulfonic acid to pH 7.4.<sup>28)</sup> The higher concentrations of NMG and

TEA were required to maintain osmolarity. In low  $Cl^-$  external solution, 140 TEA-Cl was substituted to 140 TEA-OH and titrated with methanesulfonic acid to pH 7.4. For the high BAPTA internal solution, 11 mM EGTA was replaced with 20 mM BAPTA and the concentration of NMG-Cl was reduced from 120 to 90 mM to maintain osmolarity.

## 4. Data acquisition and analysis

Voltage steps were generated and data taken using S3 (software developed by Dr. Stephen Ikeda; Guthrie Research Institute, Sayre, PA) on a Macintosh II computer (Apple Computer, Cupertino, CA). IgorPro software (WaveMetrics, Lake Oswego, OR) was used to measure current amplitudes and to fit equations (Marquardt-Levenberg algorithm) to currents and data plots.

## 5. Drugs

Test solutions were applied from a gravity-fed perfusion system with five inputs and a single output. NMG, creatine phosphate, ATP, EGTA and HEPES were obtained from Sigma Chemical Co. (St. Louis, MO).  $GDP-\beta-S$  was obtained from Boehringer Mannheim Biochemicals (Indianapolis, IN). All other chemicals were reagent grade.

# RESULTS

## 1. Calcium enhances inactivation

Calcium currents were recorded in single cells where the external solution was switched from 5 mM  $Ba^{2+}$  to 5 mM  $Ca^{2+}$ . This switch induced a 10 mV right shift in the I-V curve (Fig. 4) and decreased peak current by an average of  $58 \pm 9\%$  ( $n=43$ ). Since we were interested in the effect of  $Ca^{2+}$  on channel inactivation, we made several adjustments to compensate for the other effects of  $Ca^{2+}$ . Test voltages were depolarized 10 mV in  $Ca^{2+}$  compared to  $Ba^{2+}$  and currents in  $Ca^{2+}$  were normalized to those in  $Ba^{2+}$ . During a 5-sec depolarization to generate peak current (0 mV in  $Ba^{2+}$ , +10 mV in  $Ca^{2+}$ ) we observed more inactivation in  $Ca^{2+}$  than in  $Ba^{2+}$  (Fig. 1B). On average  $Ca^{2+}$  induced a 14 % increase in

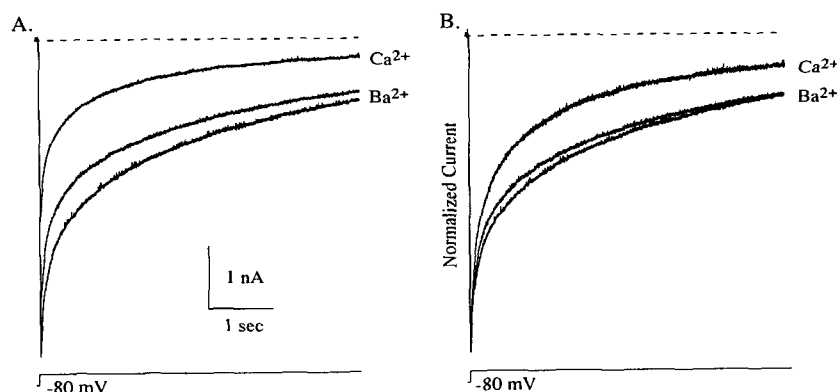


**Fig. 1.** Calcium enhances inactivation. A)  $\text{Ca}^{2+}$  current traces shown on the left were sequentially recorded in 5 mM  $\text{Ba}^{2+}$ , 5 mM  $\text{Ca}^{2+}$ , and 5 mM  $\text{Ba}^{2+}$  from the same cell. 5 sec depolarizing pulses were given from a holding potential of -80 mV to the potentials that generated peak current ( $\text{Ba}^{2+}$ : 0 mV,  $\text{Ca}^{2+}$ : 10 mV).  $\text{Ca}^{2+}$  reduced the size of peak current by 57.6% of that in  $\text{Ba}^{2+}$ . B) Current traces were normalized with respect to the peak current in  $\text{Ba}^{2+}$  to compare the time course of inactivation between  $\text{Ba}^{2+}$  and  $\text{Ca}^{2+}$ . All these recordings were made in high  $\text{Cl}^-$  solution ( $[\text{Cl}^-]_o=152$  mM,  $[\text{Cl}^-]_i = 144$  mM).

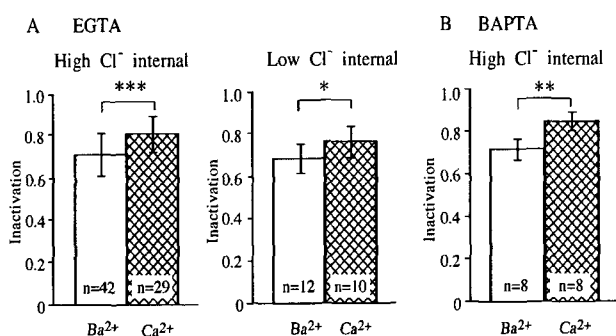


**Fig. 2.** Calcium effect was not due to calcium-activated chloride current. A) Inactivation between  $\text{Ba}^{2+}$  and  $\text{Ca}^{2+}$  were compared both in high  $\text{Cl}^-$  ( $[\text{Cl}^-]_i=144$  mM) and low  $\text{Cl}^-$  internal solution ( $[\text{Cl}^-]_i=14$  mM) in 11-mM internal EGTA. B) Inactivation between  $\text{Ba}^{2+}$  and  $\text{Ca}^{2+}$  were compared in high  $\text{Cl}^-$ , 20-mM internal BAPTA. Methanesulfonate was used to substitute for  $\text{Cl}^-$  both in external and internal solution. The magnitude of inactivation was measured as  $1 - (\text{current at the end of 5 sec} / \text{peak current})$ . Error bar represents standard deviation. ANOVA was used for statistical comparison. The inactivation was statistically different between  $\text{Ca}^{2+}$  and  $\text{Ba}^{2+}$  in both internal EGTA and in internal BAPTA. The number of cell tried is indicated. The asterisk shows significant difference (\*:  $p < 0.05$ , \*\*:  $p < 0.01$ , \*\*\*:  $p < 0.001$ ).

inactivation over  $\text{Ba}^{2+}$  (Fig. 2A) and the  $\text{Ca}^{2+}$ -induced enhancement of inactivation was observed in 37 of 39 cells.

## 2. Calcium effect was not due to Calcium activated Chloride current

In solutions in which  $\text{Cl}^-$  is the major internal and external anion, it is possible that the 5-sec depolarizations could stimulate sufficient  $\text{Ca}^{2+}$  entry to evoke the  $\text{Ca}^{2+}$ -activated  $\text{Cl}^-$  current in rat sympathetic neurons.<sup>29)</sup> If  $\text{Ca}^{2+}$ -activated  $\text{Cl}^-$  current activates slowly, the effect could masquerade as enhanced inactivation. To investigate the possible contamination by  $\text{Ca}^{2+}$ -activated  $\text{Cl}^-$  current, we substituted  $\text{Cl}^-$  internal in the internal solution with methanesulfonate to give a final  $\text{Cl}^-$  concentration 14 mM (reduced from 144 mM in our normal internal). With a constant external  $\text{Cl}^-$  of 144 mM, this substitution should change  $E_{\text{Cl}}$  from -0 mV to -60 mV, which would increase the amplitude of an outward chloride current at our test voltages (generally 0-20 mV). If  $\text{Ca}^{2+}$ -activated  $\text{Cl}^-$  current was present, the effect on calcium current would be observed as enhanced inactivation by the low  $\text{Cl}^-$  internal. However,  $\text{Cl}^-$  substitution had no effect on inactivation with either  $\text{Ca}^{2+}$  or  $\text{Ba}^{2+}$  as the charge carrier (Fig. 2A).  $\text{Ca}^{2+}$  still enhanced inactivation with the low  $\text{Cl}^-$  internal, but a comparison of inactivation between the high and low  $\text{Cl}^-$  showed no significant differences (Fig. 2A). Thus,

the  $\text{Ca}^{2+}$ -induced enhancement of inactivation did not result from contamination by  $\text{Ca}^{2+}$ -activated  $\text{Cl}^-$  current. Since the presence or absence of  $\text{Cl}^-$  did not affect inactivation, we grouped the data for analysis (Fig. 6).

Another potential problem is with our use of EGTA. First,  $\text{H}^+$  released by EGTA when it binds  $\text{Ca}^{2+}$  could acidify the cell, which has been shown to decrease N-type calcium current.<sup>30)</sup> Second, EGTA is a relatively slow  $\text{Ca}^{2+}$  buffer,<sup>11,31)</sup> so  $\text{Ca}^{2+}$  concentration near the channel could increase during our long depolarizations. The resulting reduction in driving force could mimic inactivation. To determine if these problems influenced our results, we repeated our experiments using an internal solution containing 20 mM BAPTA. As with EGTA, the inactivation was larger with  $\text{Ca}^{2+}$  than with  $\text{Ba}^{2+}$  as the charge carrier ( $n=8$ ,  $p<0.001$ ) (Fig. 2B). Thus, the  $\text{Ca}^{2+}$  induced enhancement of inactivation did not result from problems with EGTA.

### 3. Calcium enhances N-current inactivation

Though N-type calcium channel is major type in rat sympathetic neurons, non-N-type calcium current comprise 10–40% of the total current.<sup>32–34)</sup> To determine the channel type mediating the  $\text{Ca}^{2+}$  enhancement of inactivation, we used the specific N-channel blocker  $\omega$ -conotoxin GVIA ( $\omega\text{CGVIA}$ ). For the cell illustrated in Fig. 3,  $\omega\text{CGVIA}$  blocked about 80% of calcium current and on average the block was  $61\pm 12\%$  ( $n=6$ ). This value is similar to that previously published from adult rat sympathetic neurons ( $62\pm 4\%$ ).<sup>34)</sup> In 3 cells we examined the effect of  $\text{Ca}^{2+}$  on inactivation both before and after the application of  $1\ \mu\text{M}$   $\omega\text{CGVIA}$ .  $\text{Ca}^{2+}$  enhanced the inactivation of the total current (before  $\omega\text{CGVIA}$ ) by  $11\pm 7\%$  ( $n=3$ ). In the presence of toxin,  $\text{Ca}^{2+}$  still enhanced inactivation but the effect was smaller ( $6\pm 1\%$ ,  $n=3$ ) (Fig. 3D). N-current was isolated from total current by subtracting the  $\omega\text{CGVIA}$ -resistant current. The enhancement of inactivation by  $\text{Ca}^{2+}$  was larger for isolated N-current ( $13\pm 10\%$ ) (Fig. 3C) than the total current. Although small effects of  $\text{Ca}^{2+}$  were observed in the toxin resistant current, the majority of the enhancement of inactivation was due to effects of

$\text{Ca}^{2+}$  on N-type calcium channels.

### 4. Voltage dependence of inactivation

To examine the effect of  $\text{Ca}^{2+}$  on inactivation over a range of voltages we used a two pulse protocol, with 500 ms prepulses given to different voltages followed by a postpulse to a voltage producing peak inward current (usually  $+20\ \text{mV}$  in  $\text{Ca}^{2+}$  and  $+10\ \text{mV}$  in  $\text{Ba}^{2+}$ , Fig. 4). A plot of postpulse current amplitude vs. prepulse voltage revealed that maximal inactivation was observed at voltages near those yielding maximal inward current, with less inactivation at more positive and negative voltages (Fig. 4A, B). A similar U-shaped inactivation vs. voltage relationship has been observed for N-channels in other preparations.<sup>18–20)</sup>

The U-shaped voltage-dependence superficially appears to mirror the amplitude of inward current. However, superimposing the inactivation-voltage and the current-voltage (I-V) relationships shows that the inactivation curve is much broader than the I-V rela-

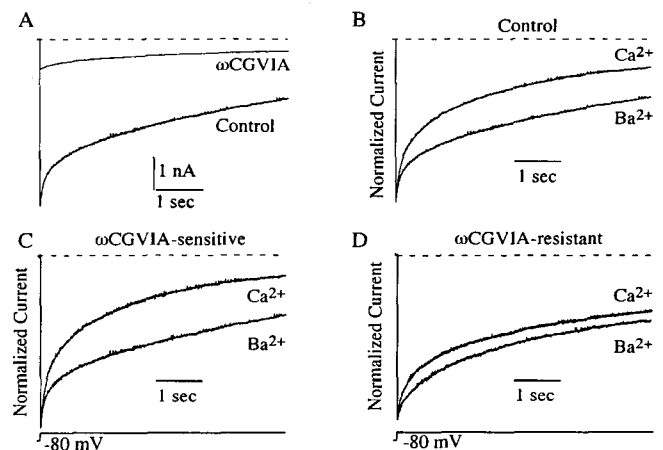


**Fig. 3.** Calcium enhances N-current inactivation. A)  $\text{Ca}^{2+}$  currents recorded with  $\text{Ba}^{2+}$  before and after  $1\ \mu\text{M}$   $\omega$ -conotoxin GVIA ( $\omega\text{CGVIA}$ ) application at the same cell with 5 sec depolarization from  $-80\ \text{mV}$  to  $0\ \text{mV}$  were shown. B) Normalized  $\text{Ca}^{2+}$  currents recorded both in  $\text{Ba}^{2+}$  and  $\text{Ca}^{2+}$  before (control, a) and after  $1\ \mu\text{M}$   $\omega\text{CGVIA}$  application ( $\omega\text{CGVIA}$ -resistant, b) at the same cell with 5 sec depolarization from  $-80\ \text{mV}$  to  $0\ \text{mV}$ ,  $10\ \text{mV}$  for  $\text{Ba}^{2+}$  and  $\text{Ca}^{2+}$ , respectively. C)  $\omega\text{CGVIA}$  sensitive N-current was isolated by subtracting the current traces of  $\omega\text{CGVIA}$ -resistant (D) from those of control in B.

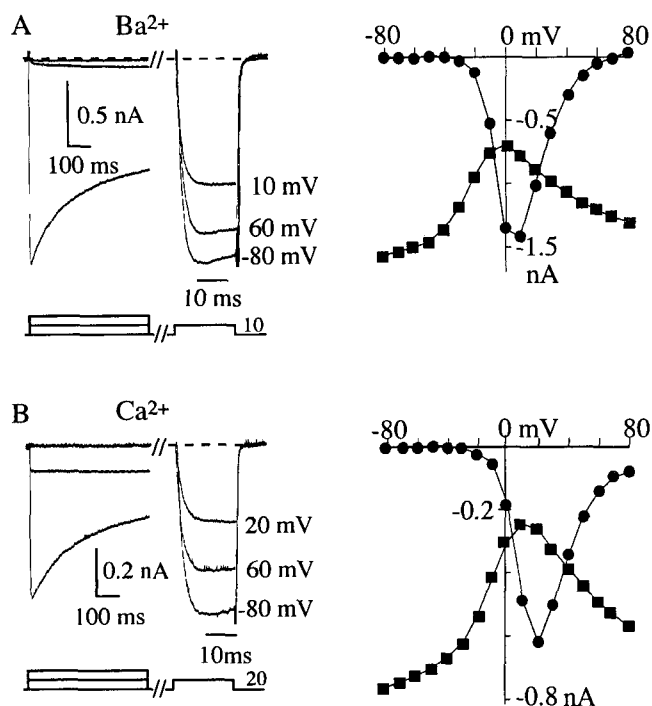


**Fig. 4.** Voltage dependence of inactivation. 500 ms depolarizing pulses of variable amplitude were given from a holding potential of  $-80$  mV to induce inactivation. This prepulse step followed by a second pulse (postpulse) to the voltage giving maximal inward current ( $+10$  mV in  $\text{Ba}^{2+}$  and  $+20$  mV in  $\text{Ca}^{2+}$ ) to assay inactivation. Data are shown for a single cell exposed to either  $\text{Ba}^{2+}$  (A) or  $\text{Ca}^{2+}$  (B). The prepulse voltage is indicated next to its corresponding current. Tail currents during the repolarization to  $-80$  mV after prepulse were omitted from the current traces during the postpulse. The internal solution contained 20 mM BAPTA. Current-voltage curves are shown with currents measured at the peak current during prepulse (I) and postpulse (n). The data points are averages of two protocols with prepulse voltages given in ascending and descending order. This was done to compensate for slow changes in current amplitude (e.g. rundown) during these long protocols.

tionship, which results from substantial inactivation at voltages yielding little or no current (Fig. 5B, C). In addition, the peak of inactivation is shifted by 10 mV to the left to of peak current in both  $\text{Ba}^{2+}$  and  $\text{Ca}^{2+}$  (Fig. 5A). While  $\text{Ca}^{2+}$  does not alter the voltage-dependence of inactivation, the magnitude of inactivation was increased during the 500 ms prepulse. For this example, maximum inactivation in  $\text{Ca}^{2+}$  was 70% compared to 55% in  $\text{Ba}^{2+}$  [mean  $62.1 \pm 0.8\%$  in  $\text{Ca}^{2+}$  ( $n=8$ ) and 44.4

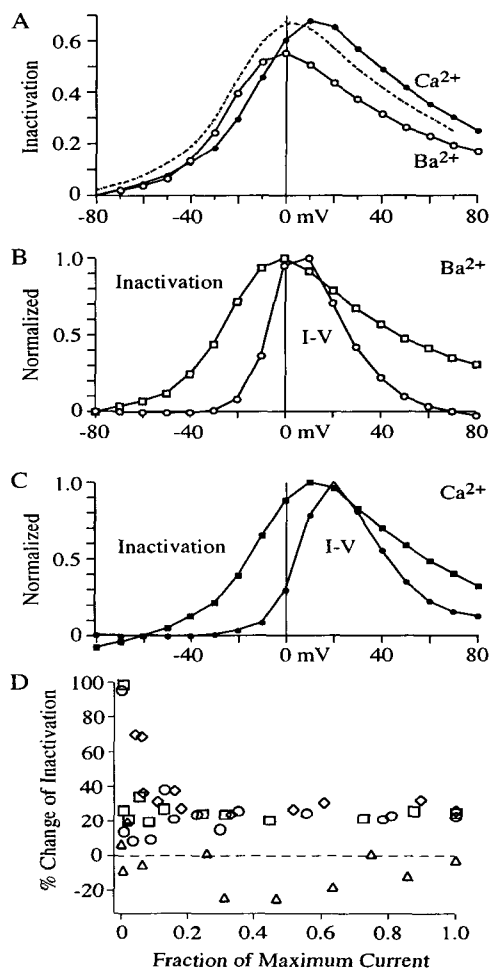


**Fig. 5.**  $\text{Ca}^{2+}$  influx is not required for the  $\text{Ca}^{2+}$  enhancement of inactivation. A) Data from the cell in Fig. 4 are replotted to show the effect of  $\text{Ca}^{2+}$  on inactivation over a range of voltages. The dashed line is the relationship in  $\text{Ca}^{2+}$  shifted 10 mV so that peak inactivation in  $\text{Ca}^{2+}$  matches that in  $\text{Ba}^{2+}$ . Note  $\text{Ca}^{2+}$  enhances inactivation at voltages with little or no  $\text{Ca}^{2+}$  current. B and C. Normalized current is superimposed on a plot of normalized inactivation vs. voltage (from the same cell in Fig. 4). Current (circle) was measured during the prepulse and was normalized to peak inward current (10 mV in  $\text{Ba}^{2+}$  or 20 mV in  $\text{Ca}^{2+}$ ). Inactivation (square) was measured from the postpulse and was normalized with respect to the maximal inactivation (inactivation at 0 mV in  $\text{Ba}^{2+}$  and 10 mV in  $\text{Ca}^{2+}$ ). D. The percent change of inactivation induced by  $\text{Ca}^{2+}$  (relative to that in  $\text{Ba}^{2+}$ ) is plotted versus prepulse voltage for 4 cells where data were obtained in both  $\text{Ca}^{2+}$  and  $\text{Ba}^{2+}$ .  $\text{Ca}^{2+}$  enhanced inactivation in 3 of 4 cells tested and in each case the enhancement was observed at voltage with no measurable  $\text{Ca}^{2+}$  current. Each different symbol ( $\circ, \square, \triangle, \diamond$ ) represents each cell recorded with voltage pulse of Fig. 4.

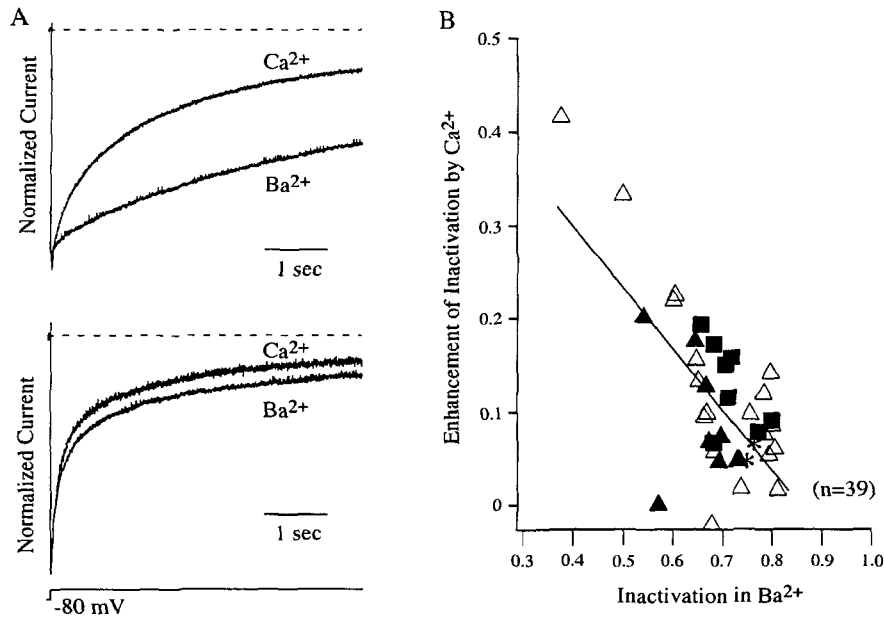


**Fig. 6.** Inverse relationship between the magnitude of inactivation in Ba<sup>2+</sup> and the enhancement of inactivation by Ca<sup>2+</sup>. A) Different cells a. and b. represent the diversity of inactivation in Ba<sup>2+</sup>. Cells were depolarized for 5 sec from -80 mV to 0 mV for Ba<sup>2+</sup> and 10 mV for Ca<sup>2+</sup>. Both cells showed more inactivation in Ca<sup>2+</sup>. B) The magnitude of inactivation in Ba<sup>2+</sup> is plotted against the enhancement of inactivation by Ca<sup>2+</sup>. Cells were pooled regardless of Cl<sup>-</sup> concentration or internal Ca<sup>2+</sup> buffer. Each different symbol represents solution with different Cl<sup>-</sup> concentration. With 11 mM internal EGTA, \* represents 21 cells recorded in the solution of [Cl<sup>-</sup>]<sub>o</sub>=152 mM, [Cl<sup>-</sup>]<sub>i</sub>=144 mM, s represents 8 cells recorded in the solution of [Cl<sup>-</sup>]<sub>o</sub>=152 mM, [Cl<sup>-</sup>]<sub>i</sub>=14 mM and \* represents 2 cells recorded in the solution of [Cl<sup>-</sup>]<sub>o</sub>=10 mM, [Cl<sup>-</sup>]<sub>i</sub>=14 mM. With 20 mM internal BAPTA, n represents 8 cells recorded in the solution of [Cl<sup>-</sup>]<sub>o</sub>=152 mM, [Cl<sup>-</sup>]<sub>i</sub>=144 mM. Straight line is the result of linear regression on all the data represented (correlation coefficient  $r = -0.73$ ,  $n=39$ ).

$\pm 0.8\%$  in Ba<sup>2+</sup> ( $n=10$ ) (Fig. 5A). Thus, Ca<sup>2+</sup> appears to enhance U-type voltage-dependent inactivation.

### 5. Two components of inactivation in both Ca<sup>2+</sup> and Ba<sup>2+</sup>

During these experiments we noticed the magnitude of inactivation measured during 5-sec steps in Ba<sup>2+</sup> varied between neurons. Fig. 6A shows two example cells that illustrate the range of inactivation. We examined the possibility that the variability of inactivation was induced by the difference of cell size or series resistance. Plots of membrane capacitance vs inactivation ( $r=0.053$ ,  $n=31$ ) and series resistance vs inactivation ( $r=-0.008$ ,  $n=31$ , data not shown) in Ba<sup>2+</sup> show-

ed no correlation. Interestingly, the effect of Ca<sup>2+</sup> on inactivation appeared to be inversely related with the magnitude of inactivation in Ba<sup>2+</sup> (Fig. 6B). This supports the idea that the same inactivation pathways are active with either Ba<sup>2+</sup> or Ca<sup>2+</sup> as the charge carrier, and if the inactivation pathways are maximally active in Ba<sup>2+</sup>, the effect of Ca<sup>2+</sup> is minimal.

The time course of inactivation during 5-sec voltage steps was nicely fitted with the sum of two exponential equations in both Ba<sup>2+</sup> and Ca<sup>2+</sup>. The exponential fits yielded amplitude and time constant for fast and slow components of inactivation. In addition, we derived the fractional amplitudes of fast and slow component relative to the total current (Fig. 7). We investigated the

effect of  $\text{Ca}^{2+}$  on each of these components by comparing amplitudes and time constants between  $\text{Ba}^{2+}$  and  $\text{Ca}^{2+}$ . Fractional amplitude of the fast component of inactivation in  $\text{Ca}^{2+}$  was significantly larger ( $0.38 \pm 0.11$ ) than that in  $\text{Ba}^{2+}$  ( $0.29 \pm 0.11$ ,  $n=31$ ,  $p < 0.001$ ). However, there was no significant difference in the fractional amplitude of slow component of inactivation between  $\text{Ba}^{2+}$  and  $\text{Ca}^{2+}$  (Fig. 7A).

Examination of the time constant showed the speed of the slow component in  $\text{Ca}^{2+}$  ( $1976.0 \pm 451.3$ ) was significantly faster than that in  $\text{Ba}^{2+}$  ( $2801.1 \pm 844.1$ ,  $n=31$ ,  $p < 0.001$ ). However, the speed of the fast component was not altered by  $\text{Ca}^{2+}$  (Fig. 7B). Although we mea-

sured a change in slow time constant, note that this value in  $\text{Ba}^{2+}$  (-3 sec) may have been limited by our 5-sec voltage step, which was less than two times longer than the calculated time constant.  $\text{Ca}^{2+}$  had differential effects on the two components of inactivation since it increased only the amplitude of the fast component and appeared to decrease only the time constant of slow component.

## 6. Time course of the $\text{Ca}^{2+}$ effect on inactivation

Much can be learned about a process by examining the speed by which it occurs. The enhancement of inactivation could result from a direct effect of  $\text{Ca}^{2+}$  on the channel or from  $\text{Ca}^{2+}$  influencing an enzymatic process (e.g. phosphorylation), which could be slow relative to  $\text{Ca}^{2+}$  directly effecting the channel. Using 100-ms

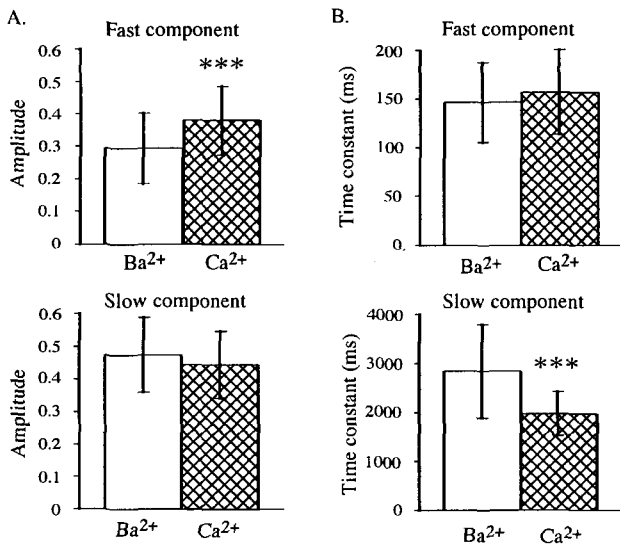


**Fig. 7.** Differential effects of  $\text{Ca}^{2+}$  on inactivation. A) Calcium enhances fractional amplitude of the fast component of inactivation. Amplitudes of inactivation between  $\text{Ba}^{2+}$  and  $\text{Ca}^{2+}$  were compared. The amplitudes of fast and slow components were calculated from double exponential fitting. The difference in the amplitude of fast component between  $\text{Ca}^{2+}$  and  $\text{Ba}^{2+}$  was significantly different ( $p < 0.001$ ), while that in amplitude of slow component was not statistically different between  $\text{Ca}^{2+}$  and  $\text{Ba}^{2+}$  ( $p > 0.05$ ). B) Calcium increases inactivation rate of slow component. Time constants of inactivation between  $\text{Ba}^{2+}$  and  $\text{Ca}^{2+}$  were compared. Time constants were obtained from the two exponential fitting of currents in  $\text{Ba}^{2+}$  and  $\text{Ca}^{2+}$ . The difference in slow time constant ( $\tau_s$ ) between  $\text{Ca}^{2+}$  and  $\text{Ba}^{2+}$  was significantly different ( $p < 0.001$ ), while that in fast time component ( $\tau_f$ ) was not statistically different between  $\text{Ca}^{2+}$  and  $\text{Ba}^{2+}$  ( $p > 0.05$ ). Error bar represents standard deviation. Paired t-test was used for statistical comparison. Total 31 cells were tested.

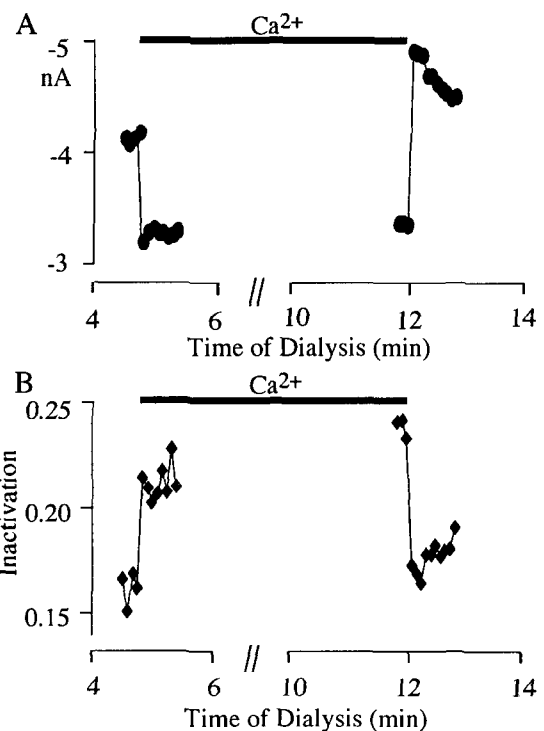


**Fig. 8.** Time course of changes in current amplitudes and inactivation. A) The switch effects from  $\text{Ba}^{2+}$  to  $\text{Ca}^{2+}$  and from  $\text{Ca}^{2+}$  to  $\text{Ba}^{2+}$  on peak calcium current were shown. B) The switch effects from  $\text{Ba}^{2+}$  to  $\text{Ca}^{2+}$  and from  $\text{Ca}^{2+}$  to  $\text{Ba}^{2+}$  on inactivation were shown. Stimulus voltage at 0 mV with 5-sec interval was used to monitor the switch effect. The line indicates the time period when the  $\text{Ca}^{2+}$  was used as charge carrier.



voltage steps, we compared the time course of effect of  $\text{Ca}^{2+}$  on current amplitude (a direct  $\text{Ca}^{2+}$  effect) with its effect on inactivation (an unknown). For the cell in Figure 8, switching from  $\text{Ba}^{2+}$  to  $\text{Ca}^{2+}$  reduced peak current to 79 % of that in  $\text{Ba}^{2+}$ . On average the current in  $\text{Ca}^{2+}$  was  $61.6 \pm 16.4$  % of that in  $\text{Ba}^{2+}$  ( $n=8$ ). The mean  $\text{Ca}^{2+}$  enhancement of inactivation in these eight cells was  $6 \pm 2\%$  ( $n=8$ ). The effect of  $\text{Ca}^{2+}$  on both current amplitude and inactivation were complete within the 5-sec interval between voltage steps. Although these observations are limited by the 5-sec interval between pulses, they illustrate that there were no profound differences between the temporal change in current amplitude and inactivation. Thus, rapid  $\text{Ca}^{2+}$  binding could be involved in both processes.

## DISCUSSION

Our main goal in this work is to establish the effect of  $\text{Ca}^{2+}$  on N-channel inactivation. We shows that  $\text{Ca}^{2+}$  can enhance calcium current inactivation and that this enhancement does not results from artifacts such as intracellular acidification or activation of  $\text{Ca}^{2+}$ -activated  $\text{Cl}^-$  current. This effect of  $\text{Ca}^{2+}$  can be ascribed to the N-type channel, which is the dominant calcium channel type in sympathetic neurons.  $\text{Ca}^{2+}$  enhances inactivation by differentially affecting two components. The amplitude of the fast component of inactivation ( $\tau = 150$  ms) was increased by  $\text{Ca}^{2+}$ , but the  $\tau_f$  was unaffected. For the slow component, the  $\tau_s$  was decreased, but the amplitude was not affected by  $\text{Ca}^{2+}$ . The main question to be address is whether either of these  $\text{Ca}^{2+}$  effects can be explained by a classic  $\text{Ca}^{2+}$ -dependent mechanism of inactivation?

### 1. $\text{Ca}^{2+}$ -dependent inactivation of L-type calcium channels

L-type calcium channels have been shown to inactivate via a  $\text{Ca}^{2+}$ -dependent mechanism. The manifestation of this mechanism is the increase in the magnitude and kinetics of inactivation upon switching from  $\text{Ba}^{2+}$  to  $\text{Ca}^{2+}$ .<sup>10, 35-37)</sup> In addition, the inactivation vs.

voltage relationship is U-shaped when  $\text{Ca}^{2+}$  is the charge carrier, with the magnitude of inactivation correlated with calcium current amplitude.<sup>10, 35, 37)</sup> Thus, it was concluded that  $\text{Ca}^{2+}$ -permeating the channels could inactivate them.<sup>38)</sup> Early work using L-type calcium channels from cardiac and smooth muscle led to the conclusion that  $\text{Ca}^{2+}$  was binding to a site on the channel that was close to the pore.<sup>10, 38-40)</sup> However, it recently has been demonstrated that calmodulin is the  $\text{Ca}^{2+}$  sensor that triggers inactivation.<sup>41, 42)</sup> The calmodulin appears to be bound to the channel so that it is close the mouth of the pore, as predicted from the earlier studies. P/Q-type channels have an analogous calmodulin binding motif, which binds calmodulin with an affinity similar to that of L-channels.<sup>37, 43)</sup> The interaction between P/Q-channels and calmodulin appears to be required for a  $\text{Ca}^{2+}$ -dependent inactivation of these channels.<sup>43, 44)</sup> Interestingly, the analogous site on N-type channels binds calmodulin very poorly.<sup>37, 45)</sup> Thus,  $\text{Ca}^{2+}$  effects on N-channel inactivation may result from a different mechanism or from calmodulin binding to a different site on the channel.

### 2. Fast N-channel inactivation

The effect of  $\text{Ca}^{2+}$  on N-channel inactivation is subtler than that on L-channel inactivation. A small enhancement of inactivation has generally been observed upon substitution of  $\text{Ba}^{2+}$  by  $\text{Ca}^{2+}$ .<sup>18, 20, 46)</sup> (Fig. 1). However, inactivation kinetics are not dramatically altered by  $\text{Ca}^{2+}$  substitution.<sup>19, 46)</sup> (Fig. 7). N-current inactivation has been shown to be kinetically complex with fast ( $\tau = 100-200$  ms) and slow ( $\tau = 1000-3000$  ms) components.<sup>19, 46)</sup> These two components can be identified in both  $\text{Ca}^{2+}$  and  $\text{Ba}^{2+}$  19,46) (Fig. 7). Thus, these properties are not consistent with a  $\text{Ca}^{2+}$ -dependent hypothesis. The  $\text{Ca}^{2+}$  effect on fast inactivation is to increase the amplitude without altering the  $\tau$  (Fig. 7). Our expectation was that the speed of inactivation would also be increased as in L-channels. Interestingly, the speed of slow inactivation was increased by  $\text{Ca}^{2+}$ , which may indicate a  $\text{Ca}^{2+}$ -dependent process (see below). One intriguing finding was that the size of the

$\text{Ca}^{2+}$  enhancement of inactivation was inversely correlated with the magnitude of inactivation in  $\text{Ba}^{2+}$ . One explanation is that the same inactivation mechanisms are active in both  $\text{Ca}^{2+}$  and  $\text{Ba}^{2+}$ . The  $\text{Ca}^{2+}$  effect is small when the inactivation pathways are maximally activated in  $\text{Ba}^{2+}$ , and the effect is larger when the pathways are not fully engaged. This idea suggests that an inactivation pathway selective for  $\text{Ca}^{2+}$  has little or no impact on N-channels. We believe this statement is true for fast inactivation, but as described below there may be a  $\text{Ca}^{2+}$ -sensitive component to slow inactivation.

One final attribute of N-channel inactivation is that the inactivation vs. voltage relationship is U-shaped in both  $\text{Ca}^{2+}$  and  $\text{Ba}^{2+}$  (Fig. 4), which is against a  $\text{Ca}^{2+}$ -dependent mechanism. The voltage steps used to generate this relationship were 500 ms in duration, which primarily isolated the fast component of inactivation ( $\tau=150$  ms). The U-shaped N-current inactivation vs. voltage relationship has been modeled as a purely voltage-dependent process.<sup>18, 20)</sup> This type of inactivation was subsequently termed U-type inactivation.<sup>23)</sup> However, a U-shaped voltage dependence of inactivation has been observed in other calcium channel types when  $\text{Ba}^{2+}$  is the charge carrier, including L-type channels ( $\alpha_{1C}$ ) expressed in tsA201 cells<sup>47)</sup> and E-class channels ( $\alpha_{1E}$ ) expressed in HEK293 cells.<sup>48)</sup> These authors raised the possibility that  $\text{Ba}^{2+}$  can activate the  $\text{Ca}^{2+}$ -dependent inactivation process in these channels. Is it possible that N-channel inactivation in  $\text{Ba}^{2+}$  results from  $\text{Ba}^{2+}$  activation of a  $\text{Ca}^{2+}$ -dependent inactivation mechanism?

### 3. U-type inactivation

Jones and Marks<sup>8)</sup> presented several arguments to discount a current-dependent mechanism for N-channel inactivation in  $\text{Ba}^{2+}$ . First, peak N-channel inactivation was consistently observed at a voltage -10 mV hyperpolarized to that generating peak current (see Fig. 5). Thus, peak current did not generate maximal inactivation. However, a similar observation has been made for L-channel inactivation in  $\text{Ca}^{2+}$ .<sup>35, 37, 49, 50)</sup> This offset of maximal inactivation from peak current has been ex-

plained within the context of a  $\text{Ca}^{2+}$ -dependent mechanism of inactivation. Noceti et al.<sup>49)</sup> were able to account for the shift by developing a model where inactivation depended on both  $\text{Ca}^{2+}$  influx and L-channel open probability. However, such a shift was predicted by a model where calmodulin was required to bind multiple  $\text{Ca}^{2+}$  ions to trigger  $\text{Ca}^{2+}$ -dependent inactivation.<sup>50)</sup> Thus, the observed shift of maximal inactivation to voltages hyperpolarized to those generating peak current can be explained by either a voltage-dependent<sup>18, 20)</sup> or  $\text{Ca}^{2+}$ -dependent<sup>49, 50)</sup> mechanism. The second argument to discount a current-dependent mechanism was the observation of significant N-channel inactivation at voltages that generated little or no current.<sup>18)</sup> This observation clearly deviates from a  $\text{Ca}^{2+}$ -dependent mechanism where inactivation requires inward calcium current.<sup>10, 35, 37)</sup> Substantial N-channel inactivation at voltages that fail to generate inward current is a consistent observation from many preparations<sup>19, 20, 46)</sup> (Fig. 5). In addition, we demonstrated that the  $\text{Ca}^{2+}$  enhancement of inactivation is not correlated with inward calcium current (Fig. 5C). Thus, the N-current inactivation vs. voltage relationship is inconsistent with a  $\text{Ca}^{2+}$ -dependent mechanism for inactivation. Finally, raising external  $\text{Ba}^{2+}$  concentration failed to increase inactivation,<sup>8, 46)</sup> as expected for a current-dependent mechanism.

Additional evidence against current dependence comes from experiments showing U-type inactivation in potassium channels.<sup>22, 23)</sup> In these experiments, the outward potassium current increases with voltage, but the inactivation shows a U-shaped voltage dependence. Together, the N-channel and potassium channel observations demonstrate that U-type inactivation is independent of current amplitude. These data are best fit by a voltage-dependent model where channels inactivate preferentially from intermediate closed states on the pathway to channel opening.<sup>20, 22, 23)</sup>

One riddle with the proposed current-dependent mechanism for inactivation in  $\text{Ba}^{2+}$ <sup>47, 48)</sup> is the mechanism by which such an effect would occur. Haack and Rosenberg<sup>36)</sup> demonstrated that fast  $\text{Ca}^{2+}$ -dependent in-

activation could not be activated in L-channels with intracellular  $Ba^{2+}$  concentrations up to 1 mM. However, fast inactivation was induced with low concentrations of internal  $Ca^{2+}$  (10  $\mu M$ ). These results are consistent with the affinity of calmodulin and other E-F hand proteins for  $Ca^{2+}$  ( $\sim 2.5 \mu M$ ) and  $Ba^{2+}$  ( $>1000 \mu M$ ).<sup>51)</sup> Thus, it appears unlikely that  $Ba^{2+}$  could activate the calmodulin-mediated  $Ca^{2+}$ -dependent mechanism of inactivation.

#### 4. Slow N-channel inactivation

During 5-sec voltage steps we were able to observe a slow component to inactivation. Exponential fitting estimated the  $\tau$  to be -3 sec in  $Ba^{2+}$  and -2 sec in  $Ca^{2+}$ . Given that the voltage step was less than 2X the slow inactivation  $\tau$  in  $Ba^{2+}$ , the derived value may be limited by the step duration. The estimate of slow inactivation  $\tau$  in  $Ca^{2+}$  should be more accurate. Since the  $\tau$  in  $Ba^{2+}$  could be larger than we estimate, the 1/3 reduction by  $Ca^{2+}$  may be an underestimate. Thus,  $Ca^{2+}$  increases the speed of slow inactivation, which is consistent with a  $Ca^{2+}$ -dependent inactivation mechanism. Previous work has generally focused on fast inactivation, since slow inactivation of N-channels is more difficult to study. However, one noteworthy study examined slow inactivation in rat sensory neurons using a 3-sec prepulse to inactivate the channels and a postpulse to assess channel availability.<sup>24)</sup> Current amplitude during the postpulse was compared when either  $Ca^{2+}$  or  $Mg^{2+}$  was present during the prepulse.  $Mg^{2+}$  was rapidly removed prior to generating the postpulse. These experiments showed significantly more inactivation when  $Ca^{2+}$  was present during the prepulse than when  $Mg^{2+}$  was present, which supported the idea that inactivation measured over seconds had a  $Ca^{2+}$ -dependent component.<sup>24)</sup>

#### 5. Hypothesized mechanism for $Ca^{2+}$ enhancement of fast inactivation

It is clear that  $Ca^{2+}$  has effects on fast inactivation, but much of the available evidence does not support a classic  $Ca^{2+}$ -dependent mechanism. To explain the N-

channel inactivation data, Patil et al.<sup>20)</sup> proposed that divalent cations are required for N-channels to undergo fast U-type inactivation. This hypothesis differs from the classic  $Ca^{2+}$ -dependent inactivation in it is the occupancy of the channels by divalent cations permits the channel to inactivate. Thus,  $Ca^{2+}$  and  $Ba^{2+}$  do not need to permeate the channel to trigger the inactivation mechanism. The enhancement of inactivation by  $Ca^{2+}$  may correspond to stronger binding of  $Ca^{2+}$  than  $Ba^{2+}$  to the channel site that permits N-channels to undergo U-type inactivation.

#### REFERENCES

1. Meir A, Ginsburg S, Butkevich A, Kachalsky SG, Kaiserman I, Ahdut R, Demircoren S, Rahamimoff R: Ion channels in presynaptic nerve terminals and control of transmitter release. *Physiol Rev* 79(3): 1019-1088 (1999)
2. Hirning LD, Fox AP, McClesky EW, et al: Dominant role of N-type Ca channels in evoked release of norepinephrine from sympathetic neurons. *Science* 239:57-61 (1988)
3. Holz GG, Dunlap K, Kream RM: Characterization of electrically-evoked release of substance P from dorsal root ganglion neurons: Methods and dihydropyridine sensitivity. *J Neurosci* 8:463-471 (1988)
4. Koh D, Hille B: Modulation by neurotransmitters of catecholamine secretion from sympathetic ganglion neurons detected by amperometry. *Proc Natl Acad Sci USA* 94:1506-1511 (1997)
5. Lipscombe D, Kongsamut S, Tsien RW:  $\alpha$ -adrenergic inhibition of sympathetic neurotransmitter release mediated by modulation of N-type calcium-channel gating. *Nature* 340:639-642 (1989)
6. Yawo H, Chuhma N: Preferential inhibition of  $\omega$ -conotoxin-sensitive presynaptic  $Ca^{2+}$  channels by adenosine autoreceptors. *Nature* 365:256-258 (1993)
7. Momiyama T, Koga E: Dopamine D2-like receptors selectively block N-type  $Ca^{2+}$  channels to reduce GABA release onto rat striatal cholinergic interneurons. *J Physiol (Lond.)* 533:479-492 (2001)
8. Forsythe ID, Tsujimoto T, Barnes-Davies M, Cuttle MF, Takahashi T: Inactivation of presynaptic calcium current contributes to synaptic depression at a fast central synapse. *Neuron* 20:797-807 (1998)
9. Fox AP: Voltage-dependent inactivation of a cal-

- cium channel. *Proc Natl Acad Sci USA* 78(2):953-956 (1981)
10. Giannattasio B, Jones SW, Scarpa A: Calcium currents in the A7r5 smooth muscle-derived cell line: calcium dependent and voltage dependent inactivation. *J Gen Physiol* 98:987-1003 (1991)
  11. Gutnick MJ, Lux HD, Swandulla D, Zucker H: Voltage-dependent and calcium-dependent inactivation of calcium channel current in identified snail neurons. *J Physiol (Lond.)* 412:197-220 (1989)
  12. Brehm E, Eckert R, Tillotson D: Calcium-mediated inactivation of calcium current in Paramecium. *J Physiol (Lond.)* 306:193-203 (1980)
  13. Brown AM, Morimoto K, Tsuda Y, Wilson DL: Calcium current-dependent and voltage-dependent inactivation of calcium channels in *Helix aspera*. *J Physiol (Lond.)* 320:193-218 (1981)
  14. Kay AR: Inactivation kinetics of Calcium current of acutely dissociated CA1 pyramidal cells of the mature guinea-pig hippocampus. *J Physiol (Lond.)* 437:27-48 (1991)
  15. Yue DT, Backx PH, Imredy JP: Ca-sensitive inactivation in the gating of single  $\text{Ca}^{2+}$  channels. *Science* 250:1735-1738 (1991)
  16. Hodgkin AL, Huxley AF: The dual effect of membrane potential on the sodium conductance in the giant axon of *Loligo*. *J Physiol (Lond.)* 116:497-506 (1952)
  17. Eckert R, Chad JE: Inactivation of Ca channels. *Progress in Biophysics and Molecular Biology* 44:215-267 (1984)
  18. Jones SW, Marks TN: Calcium currents in bullfrog sympathetic neurons: II. Inactivation. *J Gen Physiol* 94:169-182 (1989)
  19. Cox DH, Dunlap K: Inactivation of N-type calcium current in chick sensory neurons: calcium and voltage dependence. *J Gen Physiol* 104:311-336 (1994)
  20. Patil PG, Brody DL, Yue DT: Preferential closed-state inactivation of neuronal calcium channels. *Neuron* 20:1027-1038 (1998)
  21. Jones LP, DeMaria CD, Yue DT: N-type calcium channel inactivation probed by gating-current analysis. *Biophys J* 76:2530-2552 (1999)
  22. Klemic KG, Shieh C-C, Kirsch GE, Jones SW: Inactivation of Kv2.1 potassium channels. *Biophys J* 74:1779-1789 (1998)
  23. Klemic KG, Kirsch GE, Jones SW: U-type inactivation of Kv3.1 and Shaker potassium channels. *Biophys J* 81:814-826 (2001)
  24. Schroeder JE, Fischbach PS, Mamo M, McCleskey EW: Two components of high threshold  $\text{Ca}^{2+}$  current inactivate by different mechanisms. *Neuron* 5:445-452 (1990)
  25. Shirokov R: Interaction between permeant ions and voltage sensor during inactivation of N-type  $\text{Ca}^{2+}$  channels. *J Physiol (Lond.)* 518:697-703 (1999)
  26. Goo YS, Elmslie KS: Inactivation of calcium current in rat sympathetic neurons. *Society for Neuroscience Abstract*. 38:13 (1998)
  27. Ehrlich I, Elmslie KS: Neurotransmitters acting via different G proteins inhibit N-type calcium current by an identical mechanism in rat sympathetic neurons. *J Neurophysiol* 70:2251-2257 (1995)
  28. Ikeda SR: Double-pulse calcium channel current facilitation in adult rat sympathetic neurons. *J Physiol (Lond.)* 439:181-214 (1991)
  29. Sanchez-Vives MV, Gallego R: Calcium-dependent chloride current induced by axotomy in rat sympathetic neurons. *J Physiol (Lond.)* 475:391-400 (1994)
  30. Kiss L, Korn SJ: Modulation of N-type  $\text{Ca}^{2+}$  channels by intracellular pH in chick sensory neurons. *J Neurophysiol* 81:1839-1847 (1999)
  31. Neher E: Concentration profiles of intracellular calcium in the presence of a diffusible chelator. *Exp Brain Res* S14:80-96 (1986)
  32. Plummer MR, Logothetis DE, Hess P: Elementary properties and pharmacological sensitivities of calcium channels in mammalian peripheral neurons. *Neuron* 2:1453-1463 (1989)
  33. Regan LJ, Sah DWY, Bean BP:  $\text{Ca}^{2+}$  channels in rat central and peripheral neurons: High-threshold current resistant to dihydropyridine blockers and  $\omega$ -conotoxin. *Neuron* 6:269-280 (1991)
  34. Zhu Y, Ikeda SR: Adenosine modulates voltage-gated  $\text{Ca}^{2+}$  channels in adult rat sympathetic neurons. *J Neurophysiol* 70(2):610-620 (1993)
  35. Kalman D, O'Lague PH, Erxleben C, Armstrong DL: Calcium-dependent inactivation of the dihydropyridine-sensitive calcium channels in GH3 cells. *J Gen Physiol* 92:531-548 (1988)
  36. Haack JA, Rosenberg RL: Calcium-dependent inactivation of L-type calcium channels in planar lipid bilayers. *Biophys J* 66:1051-1060 (1994)
  37. Peterson BZ, DeMaria CD, Adelman JP, Yue DT: Calmodulin is the  $\text{Ca}^{2+}$  sensor for  $\text{Ca}^{2+}$ -dependent inactivation of L-type calcium channels. *Neuron* 22:549-558 (1999)
  38. Imredy JP, Yue DT: Submicroscopic  $\text{Ca}^{2+}$  diffusion mediates inhibitory coupling between individual  $\text{Ca}^{2+}$

- channels. *Neuron* 9:197-207 (1992)
39. Katzka DA, Morad M: Properties of calcium channels in guinea-pig gastric myocytes. *J Physiol (Lond.)* 413:175-197 (1989)
40. de Leon M, Wang Y, Jones L, et al: Essential  $\text{Ca}^{2+}$ -binding motif for  $\text{Ca}^{2+}$ -sensitive inactivation of L-type  $\text{Ca}^{2+}$  channels. *Science* 270:1502-1506 (1995)
41. Ehlers MD, Augustine GJ: Calmodulin at the channel gate. *Nature* 399:105-108 (1999)
42. Levitan IB: It is calmodulin after all! Mediator of the calcium modulation of multiple ion channels. *Neuron* 22:645-648 (1999)
43. Lee A, Wong ST, Gallagher D, Li B, Storm DR, Scheuer T, Catterall WA:  $\text{Ca}^{2+}$ /calmodulin binds to and modulates P/Q-type calcium channels. *Nature* 399:155-159 (1999)
44. Lee A, Scheuer T, Catterall WA:  $\text{Ca}^{2+}$ /calmodulin-dependent facilitation and inactivation of P/Q-type  $\text{Ca}^{2+}$  channels. *J Neurosci* 20:6830-6838 (2000)
45. Zuhlke RD, Pitt GS, Deisseroth K, Tsien RW, Reuter H: Calmodulin supports both inactivation and facilitation of L-type calcium channels. *Nature* 399:159-162 (1999)
46. Werz MA, Elmslie KS, and Jones SW: Phosphorylation enhances inactivation of N-type calcium channel current in bullfrog sympathetic neurons. *Pflugers Arch* 424:538-545 (1993)
47. Ferreira G, Yi J, Rios E, Shirokov R: Ion-dependent inactivation of barium current through L-type calcium channels. *J Gen Physiol* 109:449-461 (1997)
48. Jouvenceau A, Giovannini F, Bath CP, Trotman E, Sher E: Inactivation properties of human recombinant class E calcium channels. *J Neurophysiol* 83:671-684 (2000)
49. Noceti F, Olcese R, Qin N, Zhou J, Stefani E: Effect of Bay K 8644 (-) and the  $\beta 2a$  subunit on  $\text{Ca}^{2+}$ -dependent inactivation in  $\alpha_{1C}$   $\text{Ca}^{2+}$  channels. *J Gen Physiol* 111:463-475 (1998)
50. Peterson BZ, Lee JS, Mulle JG, Wang Y, de Leon M, Yue DT: Critical determinants of  $\text{Ca}^{2+}$ -dependent inactivation within an EF-hand motif of L-type  $\text{Ca}^{2+}$  channels. *Biophys J* 78:1906-1920 (2000)
51. Gu C, Cooper DMF:  $\text{Ca}^{2+}$ ,  $\text{Sr}^{2+}$ , and  $\text{Ba}^{2+}$  identify distinct regulatory sites on adenylyl cyclase (AC) type VI and VIII and consolidate the apposition of capacitative cation entry channels and  $\text{Ca}^{2+}$ -sensitive ACs. *J Biol Chem* 275:6980-6986 (2000)

## 흰쥐 교감신경 뉴론 N형 칼슘전류의 비활성화에 미치는 칼슘효과

충북의대 생리학교실\*, Tulane 의대 생리학교실†

구용숙\* · Keith S. Elmslie†

N형 칼슘전류의 비활성화 vs 전압곡선은 U형을 보인다 - 즉 칼슘 내향전류의 크기와 비활성화 정도가 어느 정도 일치한다. 이러한 U형 비활성화는 순수한 전압의존성 기전으로 설명되어져 왔으나 칼슘의존성 비활성화 기전 또한 보고되었다. 이 연구에서는 흰쥐 상행 경동맥 결절뉴론을 단일 세포로 얻은 후, whole cell patch clamp technique를 사용하여 N형 칼슘전류를 기록하고, 세포외액의 charge carrier 로서 바륨과 칼슘을 사용하면서, 칼슘이 N형 칼슘통로의 비활성화에 미치는 역할을 알아보았다. charge carrier 로 칼슘을 사용하였을 경우에 바륨을 사용하였을 때에 비하여 비활성화 정도가 증가하였으며 이러한 증가는 세포속  $Ca^{2+}$  Chelator 가 11 mM EGTA 로부터 20 mM BAPTA 로 치환되어도 계속 관찰되었다. 비활성화 vs 전압 곡선은 바륨과 칼슘 모두에서 U형이었다. charge carrier 를 칼슘으로 치환시 추가로 유도되는 비활성화 정도는 바륨사용시의 비활성화 정도와 역비례관계를 보여 두 이온에서 같은 기전으로 비활성화가 일어날 가능성을 시사하였다. 이러한 가능성을 지원해 주는 결과로 5초의 긴 저분극 자극시 바륨과 칼슘을 써서 얻은 전류기록은 2중 지수 함수로 잘 그려낼 수 있었고, 그 결과 빠른 성분(시정수: -150 ms) 과 느린 성분(시정수: -2500 ms) 를 얻었다. 칼슘이 각각의 성분에 미치는 효과는 각기 달라서 빠른 성분의 amplitude는 증가하였고 느린 성분의 시정수는 빨라졌다. 칼슘에 의해 빠른 성분의 amplitude는 증가하였으므로 이는 더 많은 채널이 빠른 경로로 비활성화되었음을 시사한다. 빠른 성분의 시정수는 변화하지 않았으므로, 이는 비활성화의 빠른 경로는 칼슘과 바륨에서 같음을 시사하며 즉 비활성화 기전이 칼슘의존성이 아님을 보여주는 증거이다. 그러나 비활성화의 느린 성분은 칼슘에 의해 그 시정수가 빨라졌으므로 칼슘의존성일 가능성이 있다.

**중심단어** : N형 칼슘전류, 비활성화, 패치클램프 테크닉, 전압의존성, 칼슘의존성, U형 비활성화